Published in final edited form as:
*Ultrasound Med Biol*. 2011 April ; 37(4): 632–641. doi:10.1016/j.ultrasmedbio.2011.01.007.

# Layer-dependent variation in the anisotropy of apparent integrated backscatter from human coronary arteries

**Joseph J. Hoffman**, **Benjamin L. Johnson**, and **Mark R. Holland**
Laboratory for Ultrasonics, Washington University, One Brookings Drive, Campus Box 1105, St. Louis, Missouri 63130

**Russell J. Fedewa** and **Anuja Nair**
Volcano Corporation, 3661 Valley Centre Drive Suite 200, San Diego, CA 92130

**James G. Miller**
Laboratory for Ultrasonics, Washington University, One Brookings Drive, Campus Box 1105, St. Louis, Missouri 63130

## Abstract

Clinical imaging of the coronary arteries in the cardiac catheterization laboratory using Intravascular Ultrasound (IVUS) is known to display a three-layered appearance, corresponding to the intima/plaque, media, and adventitia. It is not known whether ultrasonic anisotropy arising from these tissues may alter this pattern in future IVUS systems that insonify in the forward direction or obliquely. In anticipation of such devices, the current study was carried out by imaging fresh human coronary arteries in two orthogonal directions in vitro. Twenty-six sites from 12 arteries were imaged with a side-looking IVUS system, and with an acoustic microscope both radially and axially. Side-looking IVUS and radial acoustic microscopy scans demonstrated the typical “bright-dark-bright” pattern of the backscatter, with the media being significantly darker than the other two layers. Images obtained in the axial orientation exhibited a markedly different pattern, with the relative brightness of the media significantly larger than that of the intima/plaque.

### Keywords

IVUS; forward-looking; anisotropy; acoustic microscopy; backscatter; coronary; atherosclerosis; intima; media; adventitia

## Introduction

Imaging of the coronary artery tree with angiographic methods provides an approach for identifying regional narrowing presumed to reflect the presence of atherosclerotic plaque. Intravascular ultrasound (IVUS) imaging provides an approach for evaluating lesion composition and measuring plaque burden. Intracoronary catheter-based ultrasound systems are currently “side-looking” in that they generate beams that are perpendicular to the



**Corresponding Author:** James G. Miller, Ph.D., Campus Box 1105, Washington University, One Brookings Drive, St. Louis, MO 63130, voice: 314-935-6229, fax: 314-935-5868, james.g.miller@wustl.edu.

guidewire and strike the arterial wall in an approximately radial direction. Coronary arteries with an atherosclerotic plaque burden imaged in this side-looking configuration are well known to demonstrate a three-layered appearance (Nissen et al. 1991; Fitzgerald et al. 1992; Maheswaran et al. 1995). The relatively bright (echogenic) inner layer is followed by a darker (echolucent) layer, and then by another relatively bright layer. These three layers are typically interpreted as the plaque/intima, media, and adventitia, respectively.

The constituent layers of coronary arteries are known to be structurally anisotropic (Waller et al. 1992). Because the length scales of the components of these vessels are comparable to wavelengths employed in IVUS, there is reason to believe that coronary tissue may scatter anisotropically. Furthermore, because structural diversity among the layers of coronary arteries is so pronounced, each layer might express different variation of ultrasonic backscatter with insonification angle. If present, this angular dependence might cause the clinical presentation of the arterial wall layers and associated plaques to be significantly different when imaged with future IVUS catheters capable of insonifying at angles outside the limited range of current side-looking catheters. A better understanding of the impact of coronary artery anisotropy on IVUS imaging will be essential as forward-looking and oblique insonification IVUS transducers become more widely available. Such differences in layers and plaque types arising from tissue anisotropy may be useful in quantitatively characterizing zones of interest.

The impact of anisotropy on ultrasonic measurements of human arterial tissue has been explored in several previously published investigations. Picano et al. observed some differences in angle dependence among plaque types in studies of excised aortas **(**Picano et al. 1985**)**. De Kroon and collaborators examined the backscatter from excised iliac arteries as a function of angle (de Kroon et al. 1991a; de Kroon et al. 1991b). These authors observed layer-dependent variation with angle, although the experimental apparatus permitted only modest departures from the perpendicular to the vessel surface. Lockwood et al. investigated excised femoral and carotid arteries from both the radial and axial directions (Lockwood et al. 1991). A side-looking IVUS study by Hiro et al. investigated angular variation of scattering in circumferential direction (Hiro et al. 1999). To our knowledge, the present study is the first to report the anisotropy of apparent integrated backscatter between the radial and axial orientations in human coronary artery tissue.

The objective of our study was to determine how the relative level of backscatter from specific regions of coronary arteries might depend on the angle of insonification.

## Materials and Methods

### Definition of Coordinate System

As illustrated in Figure 1, arterial blood flows in what will be referred to as the axial direction, whereas a side-looking IVUS catheter interrogates tissue in what will be referred to as the radial direction. The resulting IVUS scans display two-dimensional cross-sectional images as shown in row 1 of Figure 2. Axial scans project sound along the direction of blood flow. IVUS catheters that insonify at angles between the radial and axial directions seem likely to be available soon, and imaging with such catheters is sometimes called ‘forward-looking IVUS.’ How these oblique angle IVUS systems may be impacted by the results of the current work will be addressed in the Discussion section.

### Specimen Acquisition and Preparation

Twelve human (2 female; 10 male) left anterior descending coronary arteries were collected at autopsy from individuals of age ranging from 40 to 87 with average age 53 years in compliance with regulations established by the Washington University Human Studies

Committee. From these twelve arteries, 26 sites were selected for the acoustic microscope study based on the IVUS imaging of the excised, but otherwise intact, coronary arteries as described below. Of these 26 sites, 22 were diseased with greater than 300 μm thickness of intima, and were therefore included in the full analysis presented below. Intimal layers with thicknesses less than 300 μm were too thin for axial analysis. The samples were stored in saline at all times and were refrigerated at approximately 2°C between measurements. To minimize potential changes in physical and ultrasonic properties, the samples were not frozen or chemically fixed prior to scanning (van der Steen et al. 1991; van der Steen et al. 1992; Sasaki et al. 1996; Hall et al. 2000). All scans were performed as soon as feasible, typically beginning one day after death, and always completed no later than 8 days after death. Measurements were carried out in phosphate buffered saline at 37°C.

## IVUS Studies

Side-looking intravascular ultrasound scans were performed with a catheter-based rotating single element transducer with a center frequency of 45 MHz (Revolution®, Volcano Corporation, San Diego, CA). The transducer element is rectangular and unfocused. The catheter diameter is 6F. The left anterior descending arteries were mounted in a paraffin tray and perfused with a steady flow of phosphate buffered saline at physiological temperature (37°C) and pressure (100-150 mmHg). Side branches were ligated and the vessel was cannulated to introduce the IVUS catheter. Additional details of the experimental setup have been described previously (Nair et al. 2002; Nair et al. 2007).

An IVUS scan of the entire artery was performed to identify regions of interest. Data were collected over the region of interest with an automated axial pullback that collected cross-sectional side-looking IVUS images every 0.5 mm. A representative image can be seen in the first row of Figure 2. Segments of particular interest were marked with a suture to guide subsequent acoustic microscopy studies. The suture was also visible on the IVUS image and served to confirm collocation of the acquired IVUS data.

Quantification of the IVUS images was performed by drawing regions-of-interest in the intima/plaque, media, and adventitia. The mean grayscale values were extracted from within these regions**.** Because this analysis was performed on clinical images that have been subject to pre-processing and post-processing, the extracted results are only used for relative comparisons among the IVUS data. Comparison of the absolute level of mean grayscale brightness between IVUS and acoustic microscopy results is not possible with this data set.

## Acoustic Microscopy Studies

After side-looking IVUS data had been collected, the artery was prepared for acoustic microscopy study. Figure 1 illustrates this process. First, the vessel was dissected from surrounding tissue. A micro-surgical scissors was then used to cut axially down the length of the artery, permitting it to be opened and laid flat. The artery was submerged in a bath of degassed buffered saline at 37°C, and mounted by restraining the edges of the opened artery. In this configuration, the lumen side of the artery was facing upward and presented a relatively uniform surface for ultrasonic scanning. A transverse image was created by scanning the transducer across the previously identified regions of the artery and acquiring data every 15 microns. Such a scan was made every 300 microns along the axial length of the specimen. The images made from these scans are conceptually equivalent to side-looking IVUS, because in this configuration the sound insonifies the tissue in the radial direction. These data will be referred to as radial data.

After the completion of the radial acoustic microscopy scans, the tissue sample was mounted in agarose (Sigma-Aldrich, St. Louis, MO) and cut transversely into 750 μm thick slices

with an oscillating tissue slicer (Compresstome VF-200, Precisionary Instruments, Greenville, NC). The transversely sliced samples were returned to the acoustic microscope where they were imaged again. However, this second round of imaging insonified the tissue axially and formed an image by raster scanning over the tissue and assembling the data in a C-scan fashion. The combination of radial and axial methods provides backscatter data from the same region of tissue from two orthogonal angles.

The acoustic microscope used in this study was custom built and can be operated with a wide range of transducers. In this study, a broadband single-element transducer with a nominal center frequency of 50 MHz (Panametrics V390, Olympus NDT, Waltham, MA) was employed. The transducer is focused by a lens with a diameter of 0.25” (6.35 mm), and has a focal length in water of 0.5” (12.7 mm). The beam width at the focal point is approximately 70 μm. The bandwidth used for this study extended from 30 to 60 MHz. A Newport XPS motion controller (Newport Corporation, Irvine, CA) positioned the transducer with an accuracy of better than 5 microns. The transducer was excited by a 200 ns pulse from a Panametrics 5627RPP-1 remote pulser/preamplifier (Olympus NDT, Waltham, MA) that was triggered by a Panametrics 5900 pulser (Olympus NDT, Waltham, MA). The resulting broadband ultrasound pulse was approximately 80 μm in axial spatial length. Received signals were preamplified by the Panametrics 5627RPP-1 and sent to the Panametrics 5900 for high pass (1 MHz cutoff) and low pass (100 MHz cutoff) filtering and further amplification. All data were digitized at 8 bits at 1.25 GHz, averaged 256 times, and recorded by a Tektronics 5052B oscilloscope (Tektronics Inc. Beaverton, OR) that was synchronized with the pulser. The entire system is mounted on a 1-inch thick aluminum slab for stability.

For all acoustic microscopy studies, the focal point of the transducer was placed approximately 250 microns below the surface of the tissue. A stainless steel plate was used as an ideal reference reflector. After data were collected from each sample, the steel plate was positioned at the focus of the transducer and the reflected signal recorded.

### Histology

After the completion of the ultrasonic scans, slices were fixed in 10% buffered formalin for several days. They were then embedded in paraffin, sliced, and stained with hematoxylin and eosin. Optical images of these samples were registered with the ultrasonic images to assist in the segmentation and to validate the identification of the tissue layers within the coronary arteries. Representative histology images can be seen in the fourth row of Figure 2.

### Acoustic microscope data analysis

Quantitative measurements of the local values of ultrasonic backscatter were reported in terms of apparent integrated backscatter, an imaging parameter that has been employed extensively for tissue characterization (Mimbs et al. 1981; Barzilai et al. 1987; Milunski et al. 1989; Thomas et al. 1989; Hoffmeister et al. 1995; Finch-Johnston et al. 2000; Gibson et al. 2007). Apparent integrated backscatter can be generated from diverse data sets and can be mapped to gray scale in a fashion that approximates the image mapping produced by clinical systems.

To generate integrated backscatter images an 80% Tukey window was applied to a 0.15 μs portion of the backscattered radiofrequency (RF) signal. The power spectrum of the resulting windowed segment was then computed with a Fast Fourier Transform. The power spectrum of the corresponding steel plate signal was also computed. The power spectra from the backscattered signals and from the reference signal from the steel plate were subtracted on a logarithmic scale to generate the apparent backscatter transfer function. Averaging the

apparent backscatter transfer function over the bandwidth of the transducer (30-60 MHz) yielded the apparent integrated backscatter value.

This method of calculating the apparent integrated backscatter was employed for reducing data from both the radial and axial acquisitions. However, because the tissue layers are oriented differently in the two experimental setups, radial and axial data sets require somewhat different processing.

**Radial Scan Analysis—**A radial scan insonifies intima/plaque, media, and adventitia at every scan location. The ultrasonic wave must propagate through the intima/plaque to access the media, and subsequently, through the media to access the adventitia. To construct images showing all of these layers, the radial data was analyzed in a B-scan fashion. The apparent integrated backscatter was determined at each point by systematically sliding the window along the RF trace and performing the analysis for each window position. This procedure was repeated for each RF line, and the resulting A-lines were then mapped to grayscale and assembled into a B-mode apparent integrated backscatter image. A representative radial image of a plaque-laden artery can be seen in the second row of Figure 2.

**Axial Scan Analysis—**In contrast to the radial scan, an axial scan insonifies only one type of tissue (intima/plaque, media, or adventitia) at any scan site. The axial data were analyzed by placing the front of the window at a fixed depth of approximately 200 μm for every scan site**.** By placing the front of the gate at this depth within the tissue, the analysis gate (approximately 113 μm in length) spanned the region in which the transducer's focus was placed (approximately 250 μm into the tissue). A value for apparent integrated backscatter was generated, which was assigned to the location at which the data were collected. A representative axial image of a plaque-laden artery is shown in the third row of Figure 2.

Histology images corresponding to a subset of the sites imaged were prepared and registered with the ultrasound images to guide identification of the arterial layers.

Regions-of-interest were drawn in the side-looking IVUS images and in acoustic microscope images to measure the level of apparent integrated backscatter from the layers in the coronary arteries. In each image, adventitia, media, and intima/plaque were identified. Side-looking IVUS images were segmented according to the typical three-layer interpretation. In the radial images, regions were drawn at locations where the tissue surface was as flat as possible and layers were visible. In the axial images, regions were selected for which the layers could be definitively identified. The third column of Figure 2 shows representative regions-of-interest in all of the imaging modes. The actual regions used for analysis were chosen to avoid boundaries between tissue layers, and are therefore slightly smaller than the regions in Figure 2, which were chosen for demonstrative purposes.

## Results

Figure 3 shows the trends of the apparent backscatter observed from each tissue layer in side-looking IVUS, radial acoustic microscopy, and axial acoustic microscopy. Each bar represents the mean of the 22 sites and the error bars represent standard errors. The gray scale mapping for the radial and axial images (Figure 3B**)** corresponds to the apparent integrated backscatter axis (right-side axis). The gray scale level for the IVUS images is set on the clinical system and is different from that employed for the acoustic microscope images. As described above, the clinical nature of the IVUS images prevents direct comparison with the values from acoustic microscopy, but permits comparison of the

relative scattering among the coronary artery layers. As anticipated, radial acoustic microscopy demonstrates the same relative brightness of the layers as that of a side-looking IVUS scan. In both of these modes, the typical three-layered appearance is observed, with the intima/plaque and adventitia significantly brighter than the media. However, a different trend is observed in the axial acoustic microscope images, in which the scattering from the media is much brighter than the scattering from the intima/plaque layer.

Figure 4 shows the apparent integrated backscatter for each individual site compared between layers in different orientations. The upper left panel shows the intima/plaque to media comparison in the radial orientation. Of the 22 sites, 21 exhibit smaller apparent integrated backscatter from the media than the intima/plaque. The lower left panel shows the reversal of this trend in the axial orientation, where 20 of the 22 sites demonstrate larger scattering from the media than from the intima/plaque. The upper and lower panels on the right side of Figure 4 show the comparison between the media and adventitia in the radial and axial orientations, respectively. In both orientations, the apparent integrated backscatter from the adventitia is greater than the apparent integrated backscatter from the media. In these comparisons, the individual site data points reveal that although the trends between media and adventitia are statistically significant, they seem less consistent than the trends observed between the intima/plaque and media.

Figure 5 presents the individual site data comparing the apparent integrated backscatter between the radial and axial orientations for each tissue layer. The top panel shows that the greatest anisotropy is demonstrated in the intima/plaque layer, in which the level of apparent integrated backscatter is much lower in the axial orientation than in the radial orientation. In the medial layer, shown in the middle panel of Figure 5, there is a statistically significant increase, but the individual site results suggest that there is much more variation in this trend. Many sites do increase, but a substantial number decrease, and several are essentially unchanged. The apparent integrated backscatter values from the adventitia (bottom panel of Figure 5) did not differ significantly in the radial and axial directions. The data in this panel demonstrate that the variability of the adventitia is such that a given site may demonstrate marked anisotropy, but that there appears to be no systematic anisotropy of apparent integrated backscatter in the adventitia.

Two-tailed paired T-tests were performed to verify the significance of these observations, with the results presented in Table 1 and Table 2. Table 1 shows comparisons of the different layers within each scan orientation. In both the radial and axial directions, the apparent integrated backscatter from the intima/plaque is significantly different from that of the neighboring media. The media is significantly darker than the adventitia in the radial and axial scans.

Table 2 shows the results of comparing between radial and axial in each tissue type. Differences were observed between radial and axial measurements of the apparent integrated backscatter from intima/plaque and media. No statistically significant difference was found between radial and axial scattering from adventitial tissue.

## Discussion

Side-looking IVUS scans are routinely performed in the coronary arteries to assess atherosclerosis and plaque progression, and increasingly to quantify plaque types for rupture risk evaluation. A review of the literature indicates that intravascular ultrasonic devices are being developed that will permit imaging in other orientations (Back et al. 1994; Evans et al. 1994; Gatzoulis et al. 2001; Yeh et al. 2006). When these devices become available for

clinical use, it seems likely that some of the intuitions developed from side-looking IVUS will require reevaluation (Courtney et al. 2008).

The apparent integrated backscatter images created in this study by imaging fresh coronary arteries using radial scans correspond very well with traditional side-looking IVUS images of those same arteries. One might therefore anticipate that integrated backscatter images created by axially scanning coronary arteries would provide some additional insight to the "forward-looking" IVUS catheters of the near future, which will most likely image obliquely. The results generated from the axial scans represent the extreme limits of the effects of anisotropy. Devices operating between the radial and axial orientations are therefore likely to produce backscatter values between those seen in these limiting orientations.

Specifically, this study indicates that in the axial direction, the specific coronary layers are likely to be resolvable, but will probably present quite differently than they present in the current side-looking format. The most substantial change seems likely to be in the intima/plaque layer, which is relatively echogenic in the side-looking configuration, but which demonstrates much lower backscattering in the axial direction. The results of this study indicate that the changes in the apparent backscatter from the media and adventitia are likely to be more modest, but may be significant. Although the layers produce different levels of backscatter in the axial direction than in the radial direction, the backscatter observed in the axial direction from the media is enough different than the backscatter from the intima/plaque or adventitia that there will likely be sufficient contrast to identify the internal and external elastic laminae.

As shown in Figure 3, apparent integrated backscatter from the adventitia did not differ significantly in the radial and axial directions. This finding is consistent with previous work (de Kroon et al. 1991b), and may suggest that the loose connective tissue that forms the adventitia is not preferentially oriented in the axial or radial directions.

One of the benefits that may come about from forward-looking IVUS is a potential substantial improvement in plaque quantification. One currently available method for plaque-type discrimination relies on a decision-tree method in which many spectral parameters are used to distinguish plaques (Nair et al. 2001; Nair et al. 2002). Adding an additional orientation of investigation (i.e. forward-looking IVUS), adds new parameters, and permits comparisons between radial and axial measurements of the same region. Because many of the tissues in arteries are highly directional, anisotropy is likely to be particularly useful for distinguishing tissue types. It should be noted that the axial scans of this study represent the extreme limit of angle-dependent ultrasonic imaging, and that in vivo scans would have to be executed at an oblique angle. Although the current study does not provide a direct analogy to studies at these acute angles, the significance of the changes observed over a ninety degree rotation imply that there will be a measurable impact if the imaging angle varies from normal to the arterial wall.

The measurements made in this study were of apparent integrated backscatter, a parameter that by definition is not compensated for the effects of attenuation. Therefore, the influence of attenuation should be considered when interpreting the results. The effects arising from attenuation manifest differently in the radial orientation than in the axial orientation. In the axial orientation, each tissue layer is interrogated directly, and there are, therefore, no overlying layers attenuating the signal. In the radial orientation, the intima/plaque layer is insonified directly, but measurements of the media are performed by transmitting and receiving through the intima/plaque and measurements of the adventitia are made by propagating the signal through both the intima/plaque and the media. Radial measurements

of the media and adventitia are therefore strongly influenced by attenuation from overlying tissues. This feature complicates interpretation of the results, but is pertinent to clinical imaging, because clinical images are subject to the unknown attenuation effects from overlying layers. The characteristics of apparent integrated backscatter images and clinical IVUS images reflect both the intrinsic scattering properties of the tissues and the details of the experimental configuration. For this reason, the data generated in this study are intended to indicate relative trends between layers and between orientations.

The observed relative brightness trends might be understood in terms of the orientation of the predominant directionality of the each layer relative to the insonifying beam. Many of the plaques investigated in this study were focal lesions manifest as streaks running longitudinally down the arteries. Because of this global longitudinal genesis, it is speculated that some of the structures composing the plaque have an axial preferential orientation. If this were the case, the results of this study would parallel earlier results from our lab in myocardium (Hoffmeister et al. 1995), in which insonification parallel to the predominant orientation results in less backscatter than insonification perpendicular to the predominant orientation. The media layer is primarily composed of circumferentially oriented muscle fibers, which would be approximately perpendicular to the ultrasound beam in both the radial and axial investigations. This fact may explain why the individual sites shown in the middle panel of Figure 5 do not display as consistent of a trend as the intima/plaque sites. The adventitia appears to demonstrate the least consistent trend (bottom panel of Figure 5), which suggests that the adventitia does not have structures on the scale of the wavelengths used in this study that have a preferential orientation.

The results of some aspects of this study do not appear to parallel the results of earlier work in femoral arteries (Lockwood et al. 1991). In that study, it was reported that in both the radial and axial orientations, thickened intima scattered less than media, which, in turn, scattered less than adventitia. The current work indicates that this trend holds in the axial orientation, but not in the radial orientation. This apparent disagreement is likely attributable to the many experimental differences between that work and the current study. Later work from the same group on coronary arteries (as opposed to femoral arteries) investigated radially does parallel the results of the current work and is consistent with the bright-dark-bright layered pattern seen in side-looking IVUS (Machado and Foster 2001; Machado et al. 2002).

## Limitations

The methods and therefore results of this study are subject to some practical limitations. The trends observed seem robust, but the relatively small sample size must be considered when interpreting these results. Additionally, precise preparation and positioning of minute tissue samples in very specific orientations across numerous imaging modes poses challenges to the collocation of data from these scans. The acoustic microscopy studies, which require the arteries to be opened and laid flat subjected the samples to stresses different than those to which the arteries would be exposed *in vivo*. These stresses and the resulting strains may influence the observed ultrasonic properties, including the anisotropy.

The radial and axial acoustic microscopy studies were conducted on samples whose surfaces were approximately orthogonal to the insonifying beam. Oblique imaging systems will face the additional complication of specular reflection at the interface between the blood and the plaque surface. In cases in which the plaque has an acoustic impedance similar to that of blood, the results of this study are likely to be pertinent, but in situations such as lipid-filled or calcified plaques, where the lesion’s acoustic impedance is very different from that of blood, this reflection from the surface may be a significant effect.

The time required for data collection necessitates that studies be performed over several days. No gross changes in tissue properties were observed over this period, but we cannot rule out small changes.

Because calculation of the apparent integrated backscatter does not involve compensation for diffraction effects, the different focal characteristics of the catheter-borne IVUS transducer and the acoustic microscope's transducer can impact the results. Furthermore, the diffraction field effects also differ when using the same transducer in either a radial or axial orientation. This difference arises because the same region of tissue encounters different parts of the interrogating field in each image-forming mode (B-mode for radial; C-mode for axial).

## Conclusion

Freshly excised human coronary arteries were imaged with three ultrasound modes. Two of these modes, side-looking IVUS and radial acoustic microscopy, insonify arterial tissue from the lumen through the intima into the deeper layers. Apparent integrated backscatter images made from the radial acoustic microscopy data display the same relative layer brightness as side-looking IVUS. In contrast, the third mode, axial acoustic microscopy, generated images with a reversal of the relative brightness between the media and the intima/plaque layer. This result, the magnitude of which is substantial enough to alter image appearance qualitatively, may prove to be valuable for image interpretation and tissue characterization as 'forward-looking' or oblique angle IVUS systems become clinically available.

## Acknowledgments

The authors wish to thank Stacy Amatangelo and Amanda McNeeley of Volcano Corporation for tissue preparation, IVUS imaging and histology preparation. Support for this work provided by Volcano Corporation.

## References

Back MR, Kopchok GE, White RA, Scoccianti M, Donayre CE, Maeuser H, Brener B. Forward-looking intravascular ultrasonography: in vitro imaging of normal and atherosclerotic human arteries. Am Surg. 1994; 60:738–43. [PubMed: 7944034]

Barzilai B, Saffitz JE, Miller JG, Sobel BE. Quantitative ultrasonic characterization of the nature of atherosclerotic plaques in human aorta. Circ Res. 1987; 60:459–63. [PubMed: 3555884]

Courtney BK, Munce NR, Anderson KJ, Thind AS, Leung G, Radau PE, Foster FS, Vitkin IA, Schwartz RS, Dick AJ, Wright GA, Strauss BH. Innovations in imaging for chronic total occlusions: a glimpse into the future of angiography's blind-spot. Eur Heart J. 2008; 29:583–93. [PubMed: 18238930]

de Kroon MG, van der Wal LF, Gussenhoven WJ, Bom N. Angle-dependent backscatter from the arterial wall. Ultrasound Med Biol. 1991a; 17:121–6. [PubMed: 2053208]

de Kroon MG, van der Wal LF, Gussenhoven WJ, Rijsterborgh H, Bom N. Backscatter directivity and integrated backscatter power of arterial tissue. Int J Card Imaging. 1991b; 6:265–75. [PubMed: 1919069]

Evans JL, Ng KH, Vonesh MJ, Kramer BL, Meyers SN, Mills TA, Kane BJ, Aldrich WN, Jang YT, Yock PG. Arterial imaging with a new forward-viewing intravascular ultrasound catheter, I. Initial studies. Circulation. 1994; 89:712–7. [PubMed: 8313559]

Finch-Johnston AE, Gussak HM, Mobley J, Holland MR, Petrovic O, Pérez JE, Miller JG. Cyclic variation of integrated backscatter: dependence of time delay on the echocardiographic view used and the myocardial segment analyzed. J Am Soc Echocardiogr. 2000; 13:9–17. [PubMed: 10625826]

Fitzgerald PJ, St Goar FG, Connolly AJ, Pinto FJ, Billingham ME, Popp RL, Yock PG. Intravascular ultrasound imaging of coronary arteries. Is three layers the norm? Circulation. 1992; 86:154–8. [PubMed: 1617768]

Gatzoulis L, Watson RJ, Jordan LB, Pye SD, Anderson T, Uren N, Salter DM, Fox KA, McDicken WN. Three-dimensional forward-viewing intravascular ultrasound imaging of human arteries in vitro. Ultrasound Med Biol. 2001; 27:969–82. [PubMed: 11476931]

Gibson A, Singh G, Kulikowska A, Wallace K, Hoffman J, Ludomirsky A, Holland M. Regional Variation in the Measured Apparent Ultrasonic Backscatter of Mid-Gestational Fetal Pig Hearts. Ultrasound Med Biol. 2007; 33:1955–62. [PubMed: 17689180]

Hall CS, Dent CL, Scott MJ, Wickline SA. High-frequency ultrasound detection of the temporal evolution of protein cross linking in myocardial tissue. IEEE Trans Ultrason Ferroelectr Freq Control. 2000; 47:1051–8. [PubMed: 18238640]

Hiro T, Leung CY, Karimi H, Farvid AR, Tobis JM. Angle dependence of intravascular ultrasound imaging and its feasibility in tissue characterization of human atherosclerotic tissue. Am Heart J. 1999; 137:476–81. [PubMed: 10047629]

Hoffmeister BK, Wong AK, Verdonk ED, Wickline SA, Miller JG. Comparison of the anisotropy of apparent integrated ultrasonic backscatter from fixed human tendon and fixed human myocardium. J Acoust Soc Am. 1995; 97:1307–13. [PubMed: 7876450]

Lockwood GR, Ryan LK, Hunt JW, Foster FS. Measurement of the ultrasonic properties of vascular tissues and blood from 35-65 MHz. Ultrasound Med Biol. 1991; 17:653–66. [PubMed: 1781068]

Machado JC, Foster FS. Ultrasonic integrated backscatter coefficient profiling of human coronary arteries in vitro. IEEE Trans Ultrason Ferroelectr Freq Control. 2001; 48:17–27. [PubMed: 11367784]

Machado JC, Foster FS, Gotlieb AI. Measurement of the ultrasonic properties of human coronary arteries in vitro with a 50-MHz acoustic microscope. Braz J Med Biol Res. 2002; 35:895–903. [PubMed: 12185381]

Maheswaran B, Leung CY, Gutfinger DE, Nakamura S, Russo RJ, Hiro T, Tobis JM. Intravascular ultrasound appearance of normal and mildly diseased coronary arteries: correlation with histologic specimens. Am Heart J. 1995; 130:976–86. [PubMed: 7484759]

Milunski MR, Mohr GA, Perez JE, Vered Z, Wear KA, Gessler CJ, Sobel BE, Miller JG, Wickline SA. Ultrasonic tissue characterization with integrated backscatter. Acute myocardial ischemia, reperfusion, and stunned myocardium in patients. Circulation. 1989; 80:491–503. [PubMed: 2766504]

Mimbs JW, O'Donnell M, Miller JG, Sobel BE. Detection of cardiomyopathic changes induced by doxorubicin based on quantitative analysis of ultrasonic backscatter. Am J Cardiol. 1981; 47:1056–60. [PubMed: 7223651]

Nair A, Kuban BD, Obuchowski N, Vince DG. Assessing spectral algorithms to predict atherosclerotic plaque composition with normalized and raw intravascular ultrasound data. Ultrasound Med Biol. 2001; 27:1319–31. [PubMed: 11731045]

Nair A, Kuban BD, Tuzcu EM, Schoenhagen P, Nissen SE, Vince DG. Coronary plaque classification with intravascular ultrasound radiofrequency data analysis. Circulation. 2002; 106:2200–6. [PubMed: 12390948]

Nair A, Margolis MP, Kuban BD, Vince DG. Automated coronary plaque characterisation with intravascular ultrasound backscatter: ex vivo validation. EuroIntervention. 2007; 3:113–20. [PubMed: 19737694]

Nissen S, Gurley J, Grines C, Booth D, McClure R, Berk M, Fischer C, DeMaria A. Intravascular ultrasound assessment of lumen size and wall morphology in normal subjects and patients with coronary artery disease. Circulation. 1991; 84:1087–99. [PubMed: 1884441]

Picano E, Landini L, Distante A, Salvadori M, Lattanzi F, Masini M, L'Abbate A. Angle dependence of ultrasonic backscatter in arterial tissues: a study in vitro. Circulation. 1985; 72:572–6. [PubMed: 4017209]

Sasaki H, Saijo Y, Tanaka M, Okawai H, Terasawa Y, Yambe T, Nitta S. Influence of tissue preparation on the high-frequency acoustic properties of normal kidney tissue. Ultrasound Med Biol. 1996; 22:1261–5. [PubMed: 9123651]

Thomas LJ, Barzilai B, Perez JE, Sobel BE, Wickline SA, Miller JG. Quantitative real-time imaging of myocardium based on ultrasonic integrated backscatter. IEEE Trans Ultrason Ferroelectr Freq Control. 1989; 36:466–70. [PubMed: 18285008]

van der Steen A, Cuypers M, Thijssen J. Influence of histochemical preparation on acoustic parameters of liver tissue: a 5-MHz study. Ultrasound Med Biol. 1991

van der Steen A, Thijssen J, Ebben G. Effects of tissue processing techniques in acoustical (1.2 GHz) and light microscopy. Histochem Cell Biol. 1992

Waller BF, Orr CM, Slack JD, Pinkerton CA, Van Tassel J, Peters T. Anatomy, histology, and pathology of coronary arteries: a review relevant to new interventional and imaging techniques--Part I. Clin Cardiol. 1992; 15:451–7. [PubMed: 1617826]

Yeh D, Oralkan O, Wygant I, O Donnell M, Khuri-Yakub B. 3-D ultrasound imaging using a forward-looking CMUT ring array for intravascular/intracardiac applications. IEEE Trans Ultrason Ferroelectr Freq Control. 2006; 53:1202. [PubMed: 16846153]

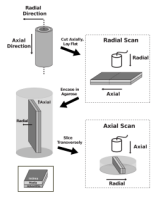


**Figure 1.**

Schematic representation of sample preparation and scanning procedure. The cylinder in the upper left image represents the fresh coronary artery from which the surrounding tissue has been removed. One side of this artery is then cut along the direction of blood flow (axially) to allow the artery to be opened and laid flat. The second image shows the flattened artery being scanned in the acoustic microscope, with sound striking the tissue radially. After the radial scan, this tissue is encased in agarose as shown in the third image and sliced transversely. The resulting sample is scanned in the acoustic microscope in an axial orientation as shown in the fourth image.

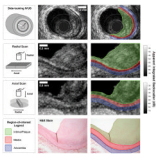

**Figure 2.**
Representative un-segmented and segmented images of one coronary artery from three ultrasound modes and histology. From top to bottom, the four rows are side-looking IVUS, radial acoustic microscopy, axial acoustic microscopy, and histology, respectively. The second column is images from each method, and the third column is the same image with **illustrative** segmentation overlaid.

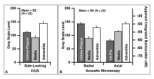

**Figure 3.**
Relative brightness **trends** of backscattering from layers of the coronary artery under three ultrasound modes. Mean gray scale level as output by the clinical side-looking IVUS system at 45 MHz (A). Backscattered brightness under acoustic microscopy with a 45 MHz center-frequency transducer (B). The gray scale value (left axis) is a linear mapping of apparent integrated backscatter relative to an ideal reflector (right axis). Because IVUS data presented in this figure were not compensated for the effects of clinical signal and image processing, only the relative trends can be compared between the left (A) and right (B) panels.

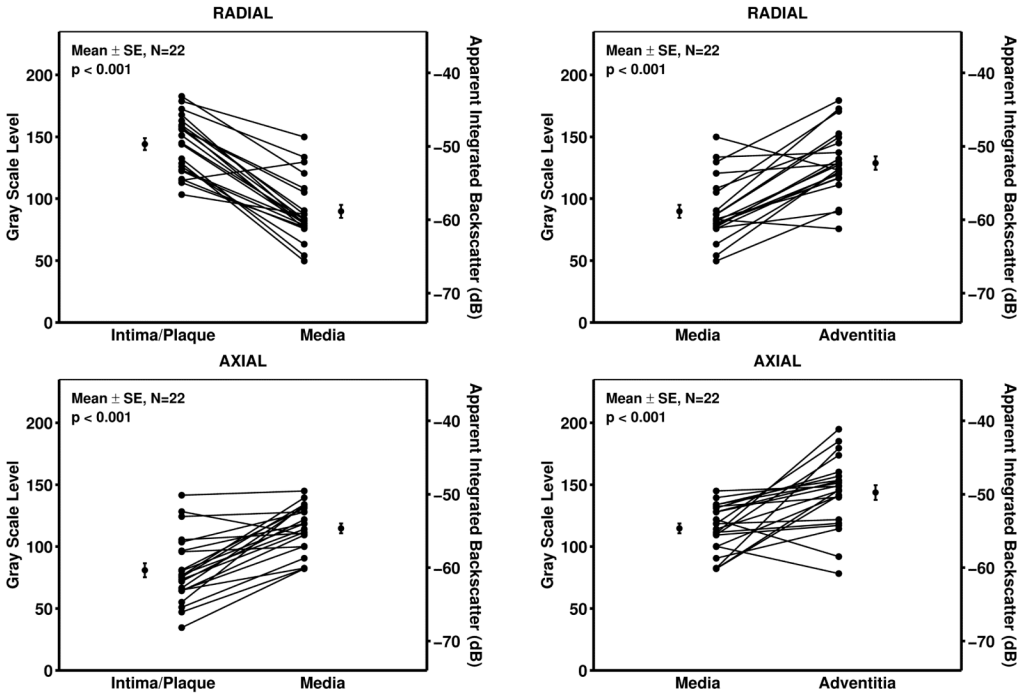


**Figure 4.**

Comparison between tissue layers of the apparent integrated backscatter from individual sites. Also shown are the mean ± standard error values for each layer. The left two panels show the comparisons between the intima/plaque and media layers for the radial (Top Left) and axial (Bottom Left) orientations. The panels on the right show the apparent integrated backscatter from the media and adventitia layers for the radial (Top Left) and axial (Bottom Left) orientations. The p-values are given for paired T-tests.

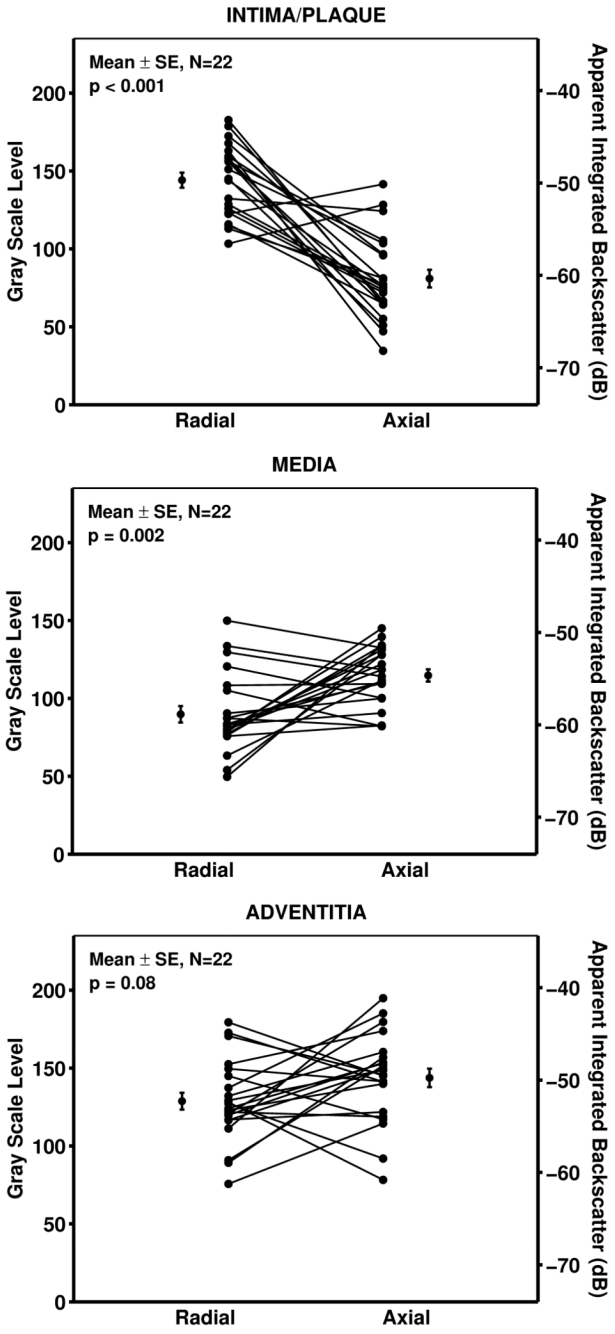


**Figure 5.**

Comparison between the radial and axial apparent integrated backscatter from individual sites within each tissue layer (Intima/Plaque, Top; Media, Middle; Adventitia, Bottom). Also shown are the mean ± standard error values for each layer. The p-values are given for paired T-tests.

## Table 1

Mean differences between the apparent integrated backscatter from layers within the coronary arteries, and the standard error of the mean of these values. The third column is the paired two-tailed T-test of these mean differences

| | Apparent Integrated Backscatter Difference | Mean Difference ± SE, N = 22 | Paired T-Test |
|---|---|---|---|
| **Radial** | Intima/Plaque - Media | 9.2 ± 0.9 dB | P < 0.001 |
| | Intima/Plaque -Adventitia | 2.6 ± 1.3 dB | P = 0.060 |
| | Media - Adventitia | −6.6 ± 1.0 dB | P < 0.001 |
| **Axial** | Intima/Plaque - Media | −5.7 ± 0.9 dB | P < 0.001 |
| | Intima/Plaque - Adventitia | −10.6 ± 1.1 dB | P < 0.001 |
| | Media - Adventitia | −4.8 ± 1.2 dB | P < 0.001 |

## Table 2

Mean differences between the apparent integrated backscatter from each tissue type in the axial and radial orientations. The third column is **the paired two-tailed** T-test of these mean differences

| Radial - Axial | Mean Difference ± SE, N = 22 | Paired T-Test |
|---|---|---|
| Intima/Plaque | 10.7 ± 1.5 dB | P < 0.001 |
| Media | −4.2 ± 1.2 dB | P = 0.002 |
| Adventitia | −2.5 ± 1.4 dB | P = 0.078 |